Effects of Ligation and Folding on Reduction Potentials of Heme Proteins

F. Akif Tezcan, Jay R. Winkler,* and Harry B. Gray*

Contribution from the Beckman Institute, California Institute of Technology, Pasadena, California 91125

Received July 17, 1998

Abstract: Ferrocytochrome *c* (Fe(II)cyt *c*) is ∼10 kcal/mol (410 meV) more stable toward unfolding than Fe(III)cyt *c*, owing mainly to the stabilization of the ferroheme by hydrophobic encapsulation and enhanced iron−methionine bonding. To determine the magnitudes of these two components, we have measured the binding constants of *N*-acetylmethionine (AcMet) and imidazole to ferric and ferrous *N*-acetylmicroperoxidase-8 (AcMP8), a heme-containing proteolytic fragment of cyt *c*. Our results show that the AcMet affinity of the heme significantly increases upon reduction, as confirmed by electrochemical measurements, and this increase accounts for 130 meV of the 410-meV stability difference between Fe(II)- and Fe(III)cyt *c*. A 240-mV upshift in reduction potential in the folded protein is attributed mainly to water exclusion from the heme environment, based on an analysis of the potentials of eight structurally characterized *c*-type cytochromes. Our analysis shows that the potentials of heme proteins can be tuned by roughly 500 mV through variations in cofactor exposure to solvent.

Introduction

The reduction potential of a metalloprotein is coupled to the folding free energies of its oxidized and reduced forms.[1−3] An upshift in the potential as a redox cofactor is moved from aqueous solution to the interior of a protein signals a greater driving force for folding the reduced form. Several factors, especially changes in cofactor inner-sphere coordination and solvation, cause the shift in potential.[1−5]

Ferrocytochrome *c* (Fe(II)cyt *c*) is ∼10 kcal/mol more stable toward unfolding than its ferric form.[6−8] This difference makes it possible to unfold the ferric protein under conditions where the ferrous protein remains folded. Electrochemical measurements demonstrate that the difference between the reduction potentials of the folded (∼260 mV) and unfolded (∼−150 mV) forms of the protein (ΔE_f) corresponds closely to the 10 kcal/mol higher stability of Fe(II)cyt *c*.[2,6,7,9] In the unfolded state of cyt *c*, the iron center is axially ligated by the imidazoles of two histidines, the native His18, and either His26 or His33, which replaces the native axial ligand, Met80.[10,11] Evidently, the heme in the unfolded protein is highly solvent exposed; the reduction potential of unfolded cyt *c* is very similar to that of bis(imidazole)-ligated iron−porphyrin species in aqueous solution (∼−200 mV).[12,13] The folding process involves the burial of the heme and the restoration of Met80 axial ligation.

To assess the contributions of heme solvation and iron ligation to ΔE_f in cyt *c*, we have examined the redox and ligand-binding properties of microperoxidase-8 (MP8), a proteolytic fragment of cyt *c* containing the heme group and amino acids 14−21. The MP8 heme is bound to the peptide backbone through thioether links to Cys14 and Cys17, and the iron is coordinated to the imidazole side chain of His18. The sixth coordination site of iron is occupied by a water or a hydroxide molecule that can be readily exchanged with other ligands. N-terminal acetylation of MP8 (AcMP8) inhibits aggregation processes that can complicate ligand-binding equilibria.[14,15] Comparison of absorption and resonance Raman (RR) spectra indicates that the *N*-acetylmethionine (AcMet) adducts of Fe(II)- and Fe(III)AcMP8 are good models for the active site of cyt *c*. As determined by binding measurements and electrochemistry, AcMet affinity for iron significantly increases upon reduction, corresponding to a large upshift in heme potential. Our finding that reduction potentials increase with decreasing heme-surface exposure for several *c*-type cytochromes suggests that water exclusion from the cofactor environment provides most of the remaining portion of ΔE_f.

(1) Churg, A. K.; Warshel, A. *Biochemistry* **1986**, *25*, 1675−1681.
(2) Bixler, J.; Bakker, G.; McLendon, G. *J. Am. Chem. Soc.* **1992**, *114*, 6938−6939.
(3) Winkler, J. R.; Wittung-Stafshede, P.; Leckner, J.; Malmström, B. G.; Gray, H. B. *Proc. Natl. Acad. Sci. U.S.A.* **1997**, *94*, 4246−4249.
(4) Gunner, M. R.; Honig, B. In *Cytochrome c*: *A Multidisciplinary Approach*; Scott, R. A., Mauk, A. G., Eds.; University Science Books: Sausalito, CA, 1996; pp 347−372.
(5) Moore, G. R.; Pettigrew, G. W. In *Cytochrome c. Evolutionary, Structural and Physicochemical Aspects*; Springer-Verlag: Heidelberg, Germany, 1990; pp 309−362.
(6) Pascher, T.; Chesick, J. P.; Winkler, J. R.; Gray, H. B. *Science* **1996**, *271*, 1558−1560.
(7) Mines, G. A.; Pascher, T.; Lee, S. C.; Winkler, J. R.; Gray, H. B. *Chem. Biol.* **1996**, *3*, 491−497.
(8) Cohen, D. S.; Pielak, G. J. *J. Am. Chem. Soc.* **1995**, *117*, 1675−1677.
(9) Hilgen-Willis, S.; Bowden, E. F.; Pielak, G. J. *J. Inorg. Biochem.* **1993**, *51*, 649−653.
(10) Elöve, G. A.; Bhuyan, A. K.; Roder, H. *Biochemistry* **1994**, *33*, 6925−6935.
(11) The pH titration of unfolded Fe(II)cyt *c* indicates a high- to low-spin transition with a midpoint at pH = 5.6, implicating bis(histidine) ligation. Telford, J. R.; Tezcan, F. A.; Gray, H. B.; Winkler, J. R. Unpublished results.
(12) Santucci, R.; Reinhard, H.; Brunori, M. *J. Am. Chem. Soc.* **1988**, *110*, 8536−8537.
(13) Chattopadhyay, K.; Mazumdar, S. *Curr. Sci.* **1997**, *73*, 65−68.
(14) Munro, O. Q.; Marques, H. M. *Inorg. Chem.* **1996**, *35*, 3752−3767.
(15) Low, D. W.; Winkler, J. R.; Gray, H. B. *J. Am. Chem. Soc.* **1996**, *118*, 117−120.

10.1021/ja982536e CCC: $15.00
Published on Web 12/08/1998

Experimental Section

Sample Preparation and Ligand Binding. All solutions were prepared with purified water (Millipore Nanopure system) and buffered to pH 7.0 with 50 mM sodium phosphate unless otherwise noted. AcMet, *N*-acetyl-L-valine (AcVal) (Sigma), DL-alanine (Ala) (Sigma), and imidazole (Aldrich) were used as received. Horse heart cyt *c* (Sigma) was oxidized with K[Co(EDTA)] and purified by FPLC (Mono S) before use. MP8 and its acetylated form were prepared and purified as previously reported.[15] AcMP8 was characterized by MALDI mass spectrometry. Concentrations of AcMP8 stock solutions were determined spectrophotometrically ($\epsilon_{396} = 157\ mM^{-1}\ cm^{-1}$). Ligand binding experiments with Fe(III)AcMP8 were performed under aerobic conditions at room temperature. Each solution contained 4−7 μM AcMP8 and up to 1.98 M AcMet, 1.68 M Ala, or 1 M imidazole. Ala and imidazole titrations were done in 200 mM phosphate buffer at pH 8 for the former and pHs 7 and 8 for the latter. Samples were allowed to equilibrate ∼30 min before spectroscopic measurements. Samples for Fe(II)AcMP8 titrations were deaerated by Ar-bubbling for 5−7 min prior to the addition of aliquots from a deaerated sodium dithionite (Mallinckrodt) stock solution. Each solution contained 4−7 μM peptide and up to 80 mM AcMet, 1.68 M Ala, or 1 M imidazole. The final concentration of dithionite in the samples was adjusted to an absorbance of 1.5−2.0 at 314 nm. Solutions were equilibrated for 10 min before recording absorption spectra (HP-8452 and Cary-14 spectrophotometers). Titration data were fit to the equation

$$A_\lambda = A_{\lambda(\mathrm{AcMP8})} - \left[\left(\frac{[\mathrm{AcMP8}]}{K_d}[\mathrm{L}]\right)\Big/\left(1 + \frac{[\mathrm{L}]}{K_d}\right)\right](\epsilon_{\lambda(\mathrm{AcMP8})} - \epsilon_{\lambda(\mathrm{L-AcMP8})})$$

where A_λ is the absorbance at a given wavelength, L is the added ligand, and $\epsilon_{\lambda(\mathrm{AcMP8})}$ and $\epsilon_{\lambda(\mathrm{L-AcMP8})}$ are the extinction coefficients of water- and ligand-bound AcMP8 at that wavelength. Fitting was optimized by adjusting $\epsilon_{\lambda(\mathrm{L-AcMP8})}$ values. The $\epsilon_{\lambda(\mathrm{AcMetAcMP8})}$ values that resulted in the best fits were used to calculate the spectra of 100% AcMet-bound Fe(II)- and Fe(III)AcMP8. Data at several wavelengths were used to calculate dissociation constants and standard deviations.

Resonance Raman Spectroscopy. Samples were 5−10 μM AcMP8. RR spectra were recorded at room temperature using a 0.75-m spectrograph (Spex 750) and a liquid nitrogen cooled CCD detector (Princeton Instruments). The 413.0-nm RR excitation was generated by a Lambda-Physik FL3002 dye laser (PBBO dye) pumped by a Lambda-Physik LPX 210I XeCl excimer laser. The excitation energy was 1−1.5 mJ, and data acquisition times ranged from 40 to 600 s at a 10-Hz repetition rate. Raman shifts were calibrated using an Ar spectral calibration lamp (Oriel).

Electrochemistry. Solutions for electrochemical measurements contained 75 μM AcMP8 and 100 mM $NaClO_4$ as supporting electrolyte in addition to 50 mM phosphate buffer (pH 7) and varying concentrations of AcMet (≤700 mM) or 100 mM imidazole. Solutions were thoroughly deaerated after the addition of each aliquot of AcMet. Measurements were conducted at room temperature with a CH Instruments 660 electrochemical workstation. A polished and sonicated 3-mm-diameter glassy carbon electrode (BAS) and a platinum wire were used as working and counter electrodes, and the reference electrode was Ag/AgCl. Cyclic voltammograms for every sample remained unchanged with repetitive scans (at scan rates up to 100 mV/s); in a typical experiment, two to four scans were recorded and the final scan was used for analysis. The anodic−cathodic peak separation (ΔE_p) was 75 mV for the imidazole complex and did not change with scan rate. Peak currents varied linearly with (scan rate)$^{1/2}$. In the methionine titration experiment, ΔE_p ranged between 80 and 120 mV depending on the methionine concentration. At low methionine concentrations, peak currents were linearly dependent on (scan rate)$^{1/2}$; at high concentrations, accurate current readings could not be obtained at a sufficient number of scan rates due to the dilution of AcMP8.

Calculation of Heme Exposure to Solvent. Solvent-exposed heme surface areas were calculated using MS[16] with a probe radius of 1.4 Å and a *Z* factor of 10 dots/Å^2. The following PDB structures were used: 1YCC (cyt *c*), 256B (cyt b_{562}), 1CYO (cyt b_5), 2C2C (cyt c_2), 2CDV (cyt c_3), 1CC5 (cyt c_5), 351C (cyt c_{551}), 1CYI (cyt c_6), 1CTM (cyt *f*), 4MBN (metmyoglobin), and 1DVH (cyt c_{553}). All were from crystal structure analyses with the exception of cyt c_{553}, for which 11 randomly selected NMR structures out of the listed 36 were used. Only monomers were considered in cases where a protein crystallized as an oligomer. A slight modification in MS was also undertaken to exclude the C_β, C_γ, O_1, and O_2 atoms of the heme propionates and the β-carbons of the vinyl substituents from calculations by evaluating them as separate residues from the heme.

(16) Connoly, M. L. *Science* **1983**, *221*, 709−713.

Results

Absorption Spectroscopy. AcMP8 is monomeric in both oxidized and reduced states at the concentrations used in this study.[17] The absorption spectrum of Fe(III)AcMP8 has been examined previously.[14,18] The spectrum of Fe(II)AcMP8 exhibits a broad Soret absorption peaking at 410 nm with a shoulder at 422 nm and Q-bands at 516 and 546 nm. A comparable Soret absorption profile in the spectrum of semisynthetic Met80Ala-Fe(II)cyt *c* (maximum at 411 nm and shoulder at 434 nm) has been interpreted in terms of a mixture of five-coordinate, high-spin and six-coordinate, low-spin iron species.[19] Similarly, the absorption spectrum of Fe(II)MP8 with an unblocked N-terminus exhibits features (Soret at 414 nm, shoulder at 430 nm, and Q-bands at 521 and 549 nm) that indicate a mixture of low- and high-spin species.[20] The low-spin component of this spectrum is possibly due to the coordination of the terminal amine group to iron. In the case of AcMP8, it is likely that a water-bound, low-spin iron is in equilibrium with a five-coordinate, high-spin species.

Ligand Binding. In the resting state, the Fe(III)AcMP8 heme is in a thermal $^5/_2$−$^1/_2$ or $^5/_2$−$^3/_2$ spin equilibrium,[21,22] with a water or a hydroxide molecule occupying the sixth coordination site of iron. The dominance of the high-spin species gives rise to a Soret band at 397 nm, broad absorption features around 500 nm, and a porphyrin (π) → iron (dπ) charge-transfer (CT) band at 622 nm (Figure 1A).[23] Upon the addition of AcMet, the spectrum of Fe(III)AcMP8 undergoes changes that are consistent with a high- to low-spin transition: the Soret band red-shifts, a Q-band emerges at 526 nm with a shoulder at 560 nm, and the 622-nm absorption drops. Further evidence for methionine S atom (S(AcMet)) coordination is provided by the presence of a band at 695 nm.[23] The isosbestic point at 404 nm implies a two-state conversion as the water is replaced by S(AcMet). The spectrum of AcMP8 remains unchanged in the

(17) Fe(III)AcMP8 does not show signs of aggregation in the concentration range used in this study (intermolecular N-terminus−Fe ligation results in a red-shifted Soret band around 404 nm (Urry, D. W.; Pettegrew, J. W. *J. Am. Chem. Soc.* **1967**, *89*, 5267−5283)); π−π stacking of the heme groups causes hypochromism of the Soret band and the appearance of a shoulder at ∼360 nm.[14] Band intensities in the spectra of Fe(II)AcMP8 and Fe(III)AcMP8 exhibit a linear dependence on concentration (≤30 μM); the spectral features do not change upon the addition of 10% MeOH (v:v), which inhibits heme aggregation.

(18) Wang, J.-S.; Tsai, A.-L.; Heldt, J.; Palmer, G.; Van Wart, H. E. *J. Biol. Chem.* **1992**, *267*, 15310−15318.

(19) Bren, K. L. Ph.D. Thesis, California Institute of Technology, 1996.

(20) Othman, S.; Le Lirzin, A.; Desbois, A. *Biochemistry* **1993**, *32*, 9781−9791.

(21) Huang, Y.-P.; Kassner, R. J. *J. Am. Chem. Soc.* **1981**, *103*, 4927−4932.

(22) Wang, J.-S.; Van Wart, H. E. *J. Phys. Chem.* **1989**, *93*, 7925−7931.

(23) Moore, G. R.; Pettigrew, G. W. In *Cytochrome c. Evolutionary, Structural and Physicochemical Aspects*; Springer-Verlag: Heidelberg, Germany, 1990; pp 27−113.

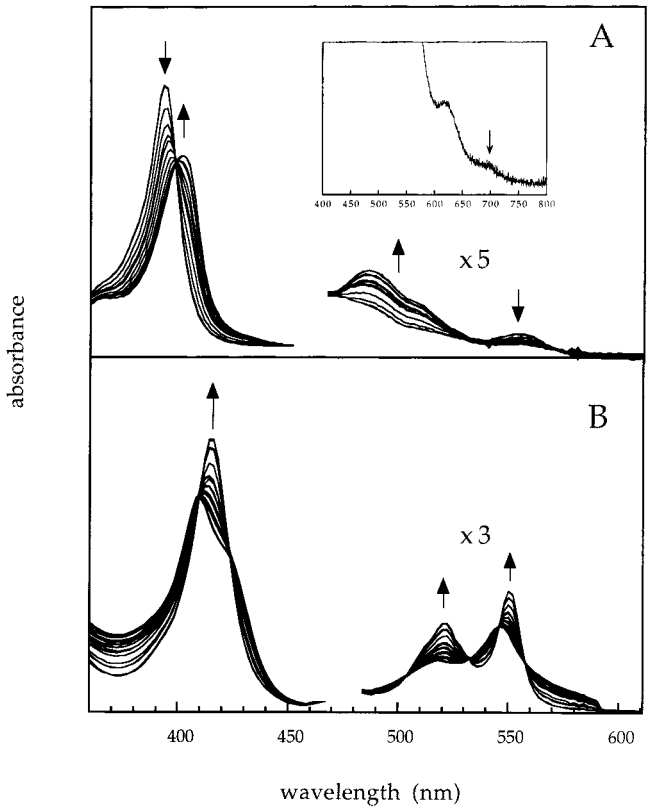

Figure 1. (a) Changes in the Fe(III)AcMP8 UV−visible absorption spectrum upon AcMet addition ([AcMet] = 0−1.98 M). (Inset) Absorption at 695 nm diagnostic of Fe(III)−S(AcMet) ligation. (b) Changes in the Fe(II)AcMP8 UV−visible absorption spectrum upon AcMet addition ([AcMet] = 0−80 mM).

presence of 1.2 M AcVal, indicating that carboxylate binding is not responsible for the AcMet-induced spin change.[24]

Similar to its oxidized counterpart, Fe(II)AcMP8 also undergoes a high- to low-spin transition upon AcMet coordination (Figure 1B). The Soret band sharpens at 415 nm, and the shoulder at 422 nm disappears. The Q-bands also become more distinct, with maxima at 520 and 550 nm, very similar to those observed in the spectrum of Fe(II)cyt *c*. Isosbestic points are evident at 410, 424, 504, 532, 546, and 558 nm. As expected from previous observations that the reduction potential of AcMP8 increases upon AcMet coordination,[25] the affinity of Fe(II)AcMP8 for AcMet is considerably higher than that of the oxidized peptide (Figure 2). Assuming a two-state equilibrium, we calculate the AcMet-dissociation constants to be 2.4 ± 0.2 mM for Fe(II)AcMP8 and 380 ± 40 mM for Fe(III)AcMP8 and that AcMet binding increases the heme reduction potential by 130 ± 15 mV (Scheme 1).

Ligation of imidazole or the N-terminus of DL-alanine to AcMP8 at pH 8 similarly results in high- to low-spin conversion, with Soret bands peaking at 406 or 405 nm for Fe(III)AcMP8 and 416 or 414 nm for Fe(II)AcMP8, respectively (see the Supporting Information). Fe(III)AcMP8 adducts of these σ-donating ligands are only slightly more stable than those of Fe(II)AcMP8 (Table 1), giving rise to a small downshift in potential (~10 mV).

(24) Munro and Marques have previously demonstrated that increasing ionic strength results in the aggregation of AcMP8.[14] We have not observed any changes in the absorption spectrum of AcMP8 associated with aggregation, even at very high AcVal concentrations.

(25) Harbury, H. A.; Cronin, J. R.; Fanger, M. W.; Hettinger, T. P.; Murphy, A. J.; Myer, Y. P.; Vinogradov, S. N. *Proc. Natl. Acad. Sci. U.S.A.* **1965**, *54*, 1658−1664.

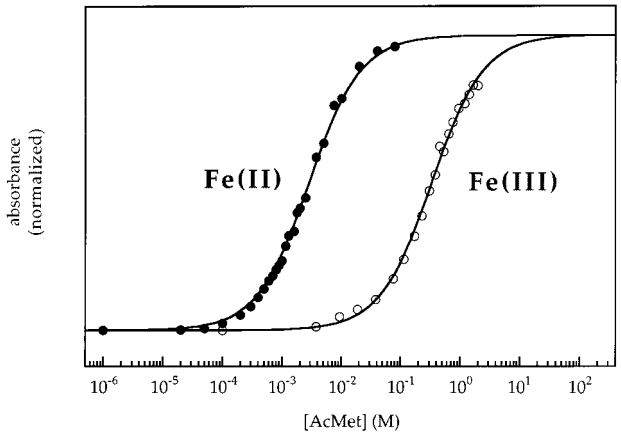

Figure 2. AcMet-binding curves for Fe(II)- and Fe(III)AcMP8 (absorbances were monitored at 416 and 408 nm, respectively).

Scheme 1. Thermodynamic Cycle of AcMP8 Reduction Potentials and AcMet Dissociation Constants

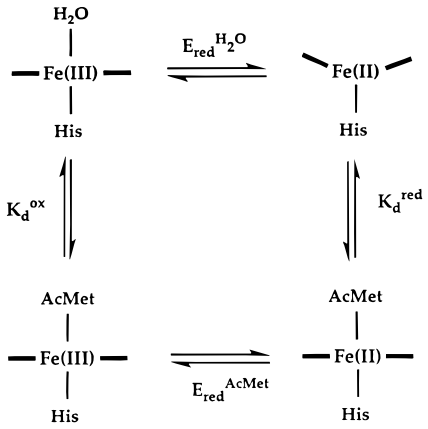

Table 1. Dissociation Constants (M) of Thioether, Imidazole, and Amine Complexes

	Fe(II)AcMP8	Fe(III)AcMP8[a]	Ru(II)$(NH_3)_5$[b]	Ru(III)$(NH_3)_5$[b]
AcMet	2.4×10^{-3}	3.8×10^{-1}	$\leq 1 \times 10^{-5}$	$\leq 6.3 \times 10^{1}$
imidazole	3.9×10^{-4} [c]	2.5×10^{-4} [c]	3.5×10^{-7}	5.3×10^{-7}
alanine	4.3×10^{-3} [c]	3.8×10^{-3} [c]	2.8×10^{-5}	6.3×10^{-6}

[a] An extensive list of binding constants for Fe(III)MP8 ligands is given in Chapter 20 of ref 4. [b] From ref 39. Corresponding entries for AcMet and alanine are $(CH_3)_2S$ and NH_3. [c] At pH 8. Dissociation contants for the imidazole adduct of AcMP8 at pH 7 are 5.8 and 3.4×10^{-4} M for Fe(II) and Fe(III) forms, respectively, in accordance with a p$K_a \sim 7$ of free imidazole.

Titration data were used to generate the absorption spectra of the AcMet complexes of ferric and ferrous AcMP8 (Figure 3). All features in these two spectra, including the maxima and the isosbestic points, agree well with those of ferric and ferrous cyt *c*. Residual absorption at 622 nm signals the presence of a small population of a high-spin species in the ferric AcMP8 complex. On the basis of magnetic measurements, Yang and Sauer also concluded that (AcMet)Fe(III)AcMP8 exists in a thermal spin equilibrium that is dominated by the low-spin form at room temperature.[26]

Resonance Raman Spectroscopy. High-frequency (1300−1650 cm^{-1}) RR spectra (Soret excitation) of heme proteins depend strongly on the oxidation state, spin state, and coordination of the metal center.[27,28] The spectrum of Fe(III)AcMP8

(26) Yang, E. K.; Sauer, K. In *Electron Transport and Oxygen Utilization*; Ho, C., Ed.; Elsevier Biomedical: New York, Amsterdam, Oxford, 1982.

(27) Spiro, T. G.; Strekas, T. C. *J. Am. Chem. Soc.* **1974**, *96*, 338−345.

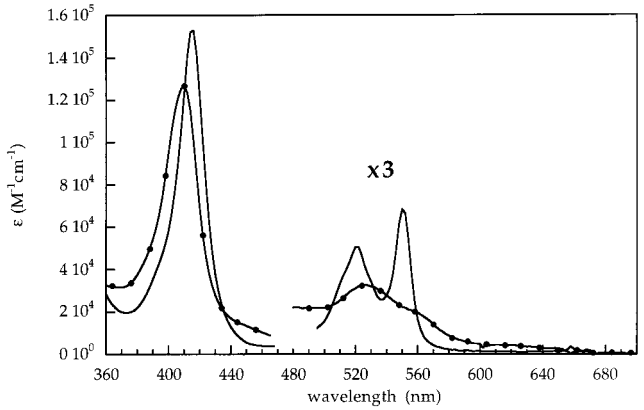

Figure 3. Calculated UV−visible absorption spectra for the AcMet complexes of AcFe(II)MP8 (straight line) and AcFe(III)MP8 (dotted line).

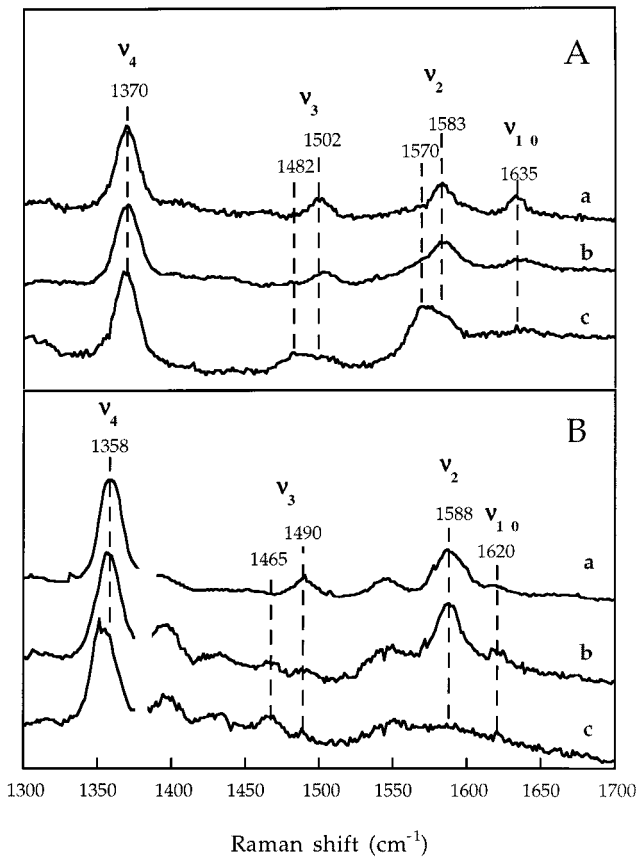

Figure 4. (A) High-frequency RR spectra of Fe(III) species: (a) Fe(III)cyt *c*; (b) Fe(III)AcMP8 in the presence of 1 M AcMet (∼70% bound); (c) Fe(III)AcMP8. (B) High-frequency RR spectra of Fe(II) species. The spectra were magnified by 150% in the range 1380−1700 cm^{-1}: (a) Fe(II)cyt *c*; (b) Fe(II)AcMP8 in the presence of 100 mM AcMet (∼97% bound); (c) Fe(II)AcMP8.

(Figure 4A) exhibits an oxidation-state marker band, ν_4, at 1370 cm^{-1}, typical of a six-coordinate Fe(III).[22,29] The porphyrin core-size marker bands (ν_3 and ν_2, centered at 1490 and 1575 cm^{-1}) are broad, owing to contributions from both high- and low-spin species. AcMet coordination to Fe(III)AcMP8 shifts ν_3 and ν_2 to 1502 and 1583 cm^{-1}, indicative of a low-spin iron center. The breadth of these bands relative to those of low-spin Fe(III)cyt *c* is most likely due to the presence of AcMet-free Fe(III)AcMP8.[30] The small high-spin population that exists even in the completely AcMet-bound AcMP8 (vide supra) should broaden the core-size marker bands as well. Due to the preservation of six-coordinate iron, the ν_4 band in (AcMet)-Fe(III)AcMP8 remains at 1370 cm^{-1}. The emergence of the ν_{10} mode at 1635 cm^{-1} further supports the presence of a low-spin, six-coordinate iron.

Fe(II)AcMP8 also appears to be an equilibrium mixture of high- and low-spin iron species, dominated by the former (Figure 4B). The ν_4 band, at 1353 cm^{-1}, is red-shifted by 5 cm^{-1} from the frequency expected for a low-spin Fe(II), consistent with observations made on high-spin, five-coordinate species such as deoxyhemoglobin.[27] The ν_3 band is split into two peaks, indicative of high- (1465 cm^{-1}) and low-spin (1490 cm^{-1}) forms of Fe(II). The spin-state-sensitive ν_{10} and ν_2 modes are too weak to be discerned, but the broad feature centered at ∼1575 cm^{-1} is evidence for a spin equilibrium. Hence, the RR spectra suggest that Fe(II)AcMP8 is a mixture of a high-spin, five-coordinate and low-spin, water-bound species at room temperature. As AcMet is added, ν_{10} and ν_2 bands can be resolved and the oxidation-state marker blue-shifts to 1357 cm^{-1}, consistent with a high- to low-spin transition. Increases in intensity at 1490 and 1588 cm^{-1} and a decrease at 1465 cm^{-1} also indicate the appearance of a low-spin species. Yet, even at an AcMet concentration of 100 mM, where the fraction of AcMet-bound AcMP8 should be greater than 97%, there is still considerable intensity at 1465 cm^{-1}. Some high-spin component also is present in the imidazole complex of Fe(II)AcMP8, which exhibits essentially the same RR spectrum (not shown). It would appear that the protein fold imposes structural constraints on Fe−S(Met) coordination, since both Fe(II)- and Fe(III)cyt *c* have low-spin ground states.

Electrochemistry. Cyclic- and square-wave voltammograms of AcMP8 in the presence of various concentrations of AcMet are consistent with binding-constant measurements (see the Supporting Information). The reduction potential of AcMP8 increases by approximately 110 mV when [AcMet] = 700 mM, whereas it remains unchanged upon the addition of up to 500 mM AcVal. Hence, S(AcMet) ligation appears to be responsible for the upshift in potential. At the AcMP8 concentrations that these measurements (75−100 μM) were performed, however, heme aggregation is apparent, as indicated by absorption spectra (not shown). Thus, the electrochemistry is complicated by the monomer/dimer equilibrium. Nevertheless, the ΔE measured electrochemically is quite close to that determined spectrophotometrically. Cyclic- and square-wave voltammetry of the AcMP8−imidazole complex ([imidazole] = 100 mM, pH 7) indicates a reduction potential 40 mV lower than that of AcMP8 (see the Supporting Information), in agreement with our titration data and a previous report on the electrochemistry of MP11 (MP8 + residues 11−13).[12]

Discussion

Cyt *c* folding involves the collapse of the polypeptide chain around the solvent-exposed heme and changes in the axial ligation of iron.[10,31−34] Burial of the heme in the hydrophobic

(28) Spiro, T. G. In *Biological Applications of Raman Spectroscopy*; Spiro, T. G., Ed.; John Wiley & Sons: New York, 1987; Vol. 3.

(29) Othman, S.; Le Lirzin, A.; Desbois, A. *Biochemistry* **1994**, *33*, 15437−15448.

(30) At the AcMet concentration used to record the spectrum in Figure 1 (1 M), the ratio of high- to low-spin species should be approximately 1:3 (K_d = 380 mM).

(31) Sosnick, T. R.; Mayne, L.; Englander, S. W. *Proteins* **1996**, *24*, 413−426.

(32) Pierce, M. M.; Nall, B. T. *Protein Sci.* **1997**, *6*, 618−627.

(33) Takahashi, S.; Yeh, S.-R.; Das, T. K.; Chan, C.-K.; Gottfried, D. S.; Rousseau, D. L. *Nat. Struct. Biol.* **1997**, *4*, 44−56.

protein matrix stabilizes the neutral Fe(II) species relative to the cationic Fe(III) form, and the reduction potential of the heme increases. The polarity of the cofactor environment has a large influence on the potential of a redox-active protein; [1,3,35−38] thus, it is not surprising that heme encapsulation provides a major portion of the 410-meV increase in the driving force for the folding of Fe(II)cyt *c*. Although the exact contribution of heme encapsulation in cyt *c* is difficult to quantify experimentally, the effects of axial ligation can be measured readily by using models such as AcMP8. A previous potentiometric measurement of the (AcMet)MP8 reduction potential suggested an upshift of ∼160 mV over that of imidazole-bound MP8.[25] At the AcMet concentrations employed in that study (≤2 M),[25] however, MP8 exists as a mixture of AcMet- and water-bound species. Indeed, it is very challenging to measure directly the reduction potential of (AcMet)MP8, due to the fact that 2 M is close to the solubility limit of AcMet. Moreover, MP8 aggregation complicates ligand-binding equilibria. Determination of the reduction-potential shift based on dissociation constants of (AcMet)Fe(II)- and (AcMet)-Fe(III)AcMP8 circumvents the complications associated with direct electrochemical measurements.

Our spectrophotometric titrations confirm that AcMet has substantially greater affinity for Fe(II) than for Fe(III). A similar pattern was observed for the binding of thioether ligands to ruthenium−ammine complexes (Table 1).[39] The difference in affinity between Fe(II)- and Fe(III)AcMP8 for AcMet corresponds to a 130-mV increase in the heme reduction potential.[40] Imidazole ligation to MP8 causes a 40-mV downshift in the potential; thus, replacing imidazole with AcMet should result in an upshift of 170 mV, in good agreement with the findings of Harbury et al.[25] and Marchon et al.,[35] who observed a 168-mV upshift with a synthetic heme model system. This value indicates that encapsulation of the heme by the protein raises the cyt *c* potential by ∼240 mV.

Tuning the Fe(III/II) potential in heme proteins is critical for function. It has been a continuing challenge for theory and experiment to understand how the protein structure regulates this potential.[41−44] Site-directed mutagenesis experiments have revealed the roles of individual amino acid side chains in this regulation,[45−54] and theoretical calculations have focused on the electrostatic heme−protein and heme−solvent interactions in an attempt to account for the potential shifts caused by heme encapsulation.[1,55−57] In an analysis of eight structurally characterized *c*-type cytochromes, we have found that the reduction potential increases with decreasing heme exposure to solvent (Figure 5).[58,59] The C_β, C_γ, O_1, and O_2 atoms of the heme propionates and the β-carbons of the vinyl groups were excluded from the solvent-exposed surface-area calculations in order to limit the analysis to the conjugated porphyrin ring system and atoms within one σ-bond from the ring. Heme potentials were corrected by converting His-His ligated hemes (hemes 1−4 and 11) to His-Met coordination through the addition of 170 mV to the reported values.[60] The potentials of the four hemes of cyt c_3 (hemes 1−4), which were not included in the correlation, lie significantly higher than a linear potential/exposure model would predict. These hemes are more exposed to the solvent environment than are the cofactors in most other proteins, owing to the relatively small size of cyt c_3 (107 amino acids). It would

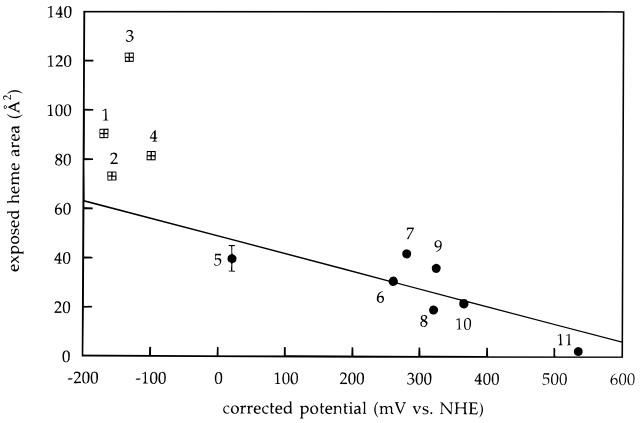

Figure 5. Solvent-exposed heme area vs corrected reduction potential: (1−4) hemes 4-1, cyt c_3 (*D. vulgaris* Miyazaki F);[61] (5) cyt c_{553} (*D. vulgaris*, average of 11 solution structures);[62] (6) cyt *c* (*S. cerevisiae*);[5] (7) cyt c_{551} (*P. aeruginosa*);[63] (8) cyt c_5 (*A. vinelandii*);[64] (9) cyt c_2 (*R. rubrum*);[63] (10) cyt c_6 (*C. reinhardtii*);[65] (11) cyt *f* (turnip).[66]

(34) Telford, J. R.; Wittung-Stafshede, P.; Gray, H. B.; Winkler J. R. *Acc. Chem. Res.* **1998**, *31*, 755−763.
(35) Marchon, J.-C.; Mashiko, T.; Reed, C. A. In *Electron Transport and Oxygen Utilization*; Ho, C., Ed.; Elsevier Biomedical: New York, Amsterdam, Oxford, 1982.
(36) Stephens, P. J.; Jollie, D. R.; Warshel, A. *Chem. Rev.* **1996**, *96*, 2491−2513.
(37) Kassner, R. J. *Proc. Natl. Acad. Sci. U.S.A.* **1972**, *69*, 2263−2267.
(38) Kassner, R. J. *J. Am. Chem. Soc.* **1973**, *95*, 2674−2677.
(39) Kuehn, C. G.; Taube, H. *J. Am. Chem. Soc.* **1976**, *98*, 689−702.
(40) Wilgus et al. (Wilgus, H.; Ranweiler, J. S.; Wilson, G. S.; Stellwagen, E. *J. Biol. Chem.* **1978**, *253*, 3265−3272) reported that methionine binding affinities of several heme-containing cyt *c* fragments were up to 2 orders of magnitude greater for the ferrous derivatives, and they were pH dependent between pH 3.1 and 7.0, at least in part due to competitive ligation by histidines present in these protein fragments. Binding affinities for both oxidation states were only reported at pH 4.8, where they were 99 and 3.9 M^{-1} for the ferrous and ferric forms, respectively, corresponding to a reduction potential increase of ∼80 mV.
(41) Zhou, H.-X. *J. Biol. Inorg. Chem.* **1997**, *2*, 109−113.
(42) Mauk, A. G.; Moore, G. R. *J. Biol. Inorg. Chem.* **1997**, *2*, 119−125.
(43) Gunner, M. R.; Alexov, E.; Torres, E.; Lipovaca, S. *J. Biol. Inorg. Chem.* **1997**, *2*, 126−134.
(44) Warshel, A.; Papazyan, A.; Muegge, I. *J. Biol. Inorg. Chem.* **1997**, *2*, 143−152.
(45) Varadarajan, R.; Zewert, T. E.; Gray, H. B.; Boxer, S. G. *Science* **1989**, *243*, 69−72.
(46) Lloyd, E.; King, B. C.; Hawkridge, F. M.; Mauk, A. G. *Inorg. Chem.* **1998**, *37*, 2888−2892.
(47) Davies, A. M.; Guillemette, J. G.; Smith, M.; Greenwood, C.; Thurgood, A. G. P.; Mauk, A. G.; Moore, G. R. *Biochemistry* **1993**, *32*, 5431−5435.
(48) Cutler, R. L.; Davies, A. M.; Creighton, S.; Warshel, A.; Moore, G. R.; Smith, M.; Mauk, A. G. *Biochemistry* **1989**, *28*, 3188−3197.
(49) Whitford, D.; Gao, Y.; Pielak, G. J.; Williams, R. J. P.; McLendon, G. L.; Sherman, F. *Eur. J. Biochem.* **1991**, *200*, 359−367.
(50) Rafferty, S. P.; Pearce, L. L.; Barker, P. D.; Guillemette, J. G.; Kay, C. M.; Smith, M.; Mauk, A. G. *Biochemistry* **1990**, *29*, 9365−9369.
(51) Louie, G. V.; Pielak, G. J.; Smith, M.; Brayer, G. D. *Biochemistry* **1988**, *27*, 7870−7876.
(52) Rodgers, K. K.; Sligar, S. G. *J. Am. Chem. Soc.* **1991**, *113*, 9419−9421.
(53) Guillemette, J. G.; Barker, P. D.; Eltis, L. D.; Lo, T. P.; Smith, M.; Brayer, G. D.; Mauk, A. G. *Biochimie* **1994**, *76*, 592−604.
(54) Rivera, M.; Seetharaman, R.; Girdhar, D.; Wirtz, M.; Zhang, X.; Wang, X.; White, S. *Biochemistry* **1998**, *37*, 1485−1494.
(55) Langen, R.; Brayer, G. D.; Berghuis, A. M.; McLendon, G.; Sherman, F.; Warshel, A. *J. Mol. Biol.* **1992**, *224*, 589−600.
(56) Gunner, M. R.; Honig, B. *Proc. Natl. Acad. Sci. U.S.A.* **1991**, *88*, 9151−9155.
(57) Zhou, H.-X. *J. Am. Chem. Soc.* **1994**, *116*, 10362−10375.
(58) In a similar analysis, E. Stellwagen (*Nature* **1978**, *275*, 73−74) examined the reduction potentials of six structurally characterized *b*- and *c*-type heme proteins without correcting for axial ligation effects. He concluded that the principal determinant of reduction potential is heme exposure to solvent.
(59) In *c*-type cytochromes, the porpyhrin is covalently linked to two cysteines through the vinyl substituents on the ring, while in *b*-type cytochromes, there is no covalent attachment between the peptide backbone and the porphyrin. An extended correlation including *b*-type hemes is given in the Supporting Information.

appear that the downshift of the potential with increasing heme exposure reaches a limit somewhere in the 60−100 Å^2 range. Further evidence for this limit are the high potentials of hemes in MP8, unfolded cyt *c*, and the alkaline form of cyt *c* (20 to −50 mV after ligand correction),[67] which are presumably solvent-exposed to a great extent.

Cyt *f* is at the high-potential end of the correlation; its heme has a solvent exposure very close to zero (2.5 Å^2) and a corrected potential of 535 mV, significantly higher than the next set of potentials (hemes 6−10). When the heme propionates and the vinyl β-carbons are included in the calculations, the solvent exposure of the cyt *f* heme (51 Å^2) is not significantly lower than those of hemes 6−10. Apparently, by burying the conjugated portion of the porphyrin ring almost completely, the protein is able to achieve a very high reduction potential.[68] We believe that 600 mV should be close to the maximum attainable potential of a His-Met ligated protein.

According to our examination, reduction potentials of *c*-type cytochromes can be tuned by roughly 500 mV through variations in the heme exposure to solvent. Several investigations have shown that electrostatic interactions other than those between the heme and the solvent also play a role in tuning the potentials,[41−44] which is evidenced by the scatter in Figure 5. Since changes in axial ligation have been shown to shift the potential by as much as 650 mV,[69] a protein can cover a 1-V range by proper adjustment of the heme environment within its folded structure.

Acknowledgment. We thank B. R. Crane for assistance with MS calculations and J. R. Telford and D. W. Low for helpful discussions. H.B.G. thanks Balliol College and the Inorganic Chemistry Laboratory, University of Oxford, for providing a stimulating environment during 1997−98. This work was supported by the NSF (Grant MCB-9630465) and the Arnold and Mabel Beckman Foundation.

Supporting Information Available: Figures showing time dependence of the absorption spectrum of Fe(II)AcMP8, concentration dependence of the absorption spectra of Fe(II)- and Fe(III)AcMP8, absorption data for the imidazole and DL-alanine titrations of AcMP8, RR spectrum of the imidazole complex of Fe(II)AcMP8, changes in the CV of AcMP8 upon AcMet and imidazole binding, and heme exposure vs potential correlations (10 pages, print/PDF). See any current masthead page for ordering information and Web access instructions.

JA982536E

(60) The effect of the amine-terminus ligation on the heme potential in cyt *f* was considered to be the same as that of histidine ligation. Our electrochemical measurements indicate that ligation of the alanine methyl ester N-terminus downshifts the AcMP8 reduction potential by ∼40 mV.

(61) The four microscopic (interaction-decoupled) heme potentials in cyt c_3 were reported by Fan et al. (Fan, K.; Akutsu, H.; Kyogoku, Y.; Niki, K. *Biochemistry* **1990**, *29*, 2257−2263). The assignment of these potentials to individual hemes was made by Park et al. (Park, J.-S.; Kano, K.; Niki, K.; Akutsu, H. *FEBS Lett.* **1991**, *285*, 149−151).

(62) Blackledge, M. J.; Guerlesquin, F.; Marion, D. *Proteins* **1996**, *24*, 178−194.

(63) Taniguchi, V. T.; Sailasuta-Scott, N.; Anson, F. C.; Gray, H. B. *Pure Appl. Chem.* **1980**, *52*, 2275−2281.

(64) Mathews, F. S. *Prog. Biophys. Mol. Biol.* **1984**, *45*, 1−56.

(65) Kerfeld, C. A.; Anwar, H. P.; Interrante, R.; Merchant, S.; Yeates, T. O. *J. Mol. Biol.* **1995**, *250*, 627−647.

(66) Cramer, W. A.; Whitmarsh, J. *Annu. Rev. Plant Physiol.* **1977**, *28*, 133−172.

(67) Barker, P. D.; Mauk, A. G. *J. Am. Chem. Soc.* **1992**, *114*, 3619−3624.

(68) Our correlation, therefore, provides a possible solution to the "cyt *f* puzzle" in the Mauk−Moore commentary.[42]

(69) This value is from work on position-80 mutants of cyt *c* (Raphael, A. L.; Gray, H. B. *J. Am. Chem. Soc.* **1991**, *113*, 1038−1040).